
Evaluating the temporal understanding of neural networks on event-based action recognition with DVS-Gesture-Chain

Alex Vicente-Sola¹, Davide L. Manna¹, Paul Kirkland¹, Gaetano Di Caterina¹, and Trevor Bihl²

¹ Neuromorphic Sensor Signal Processing Lab, Centre for Image and Signal Processing, Electrical and Electronic Engineering, University of Strathclyde, Glasgow, UK

² Air Force Research Laboratory, Wright Patterson AFB, OH
alex.vicente-sola@strath.ac.uk

Abstract

Enabling artificial neural networks (ANNs) to have temporal understanding in visual tasks is an essential requirement in order to achieve complete perception of video sequences. A wide range of benchmark datasets is available to allow for the evaluation of such capabilities when using conventional frame-based video sequences. In contrast, evaluating them for systems targeting neuromorphic data is still a challenge due to the lack of appropriate datasets. In this work we define a new benchmark task for action recognition in event-based video sequences, DVS-Gesture-Chain (DVS-GC), which is based on the temporal combination of multiple gestures from the widely used DVS-Gesture dataset. This methodology allows to create datasets that are arbitrarily complex in the temporal dimension. Using our newly defined task, we evaluate the spatio-temporal understanding of different feed-forward convolutional ANNs and convolutional Spiking Neural Networks (SNNs). Our study proves how the original DVS Gesture benchmark could be solved by networks without temporal understanding, unlike the new DVS-GC which demands an understanding of the ordering of events. From there, we provide a study showing how certain elements such as spiking neurons or time-dependent weights allow for temporal understanding in feed-forward networks without the need for recurrent connections. Code available at: <https://github.com/VicenteAlex/DVS-Gesture-Chain>

1 Introduction

In the field of computer vision, temporal understanding of visual stimuli is a pivotal challenge in the path to human-level intelligence. Through the years, multiple datasets and tasks have been created in order to evaluate this capability in artificial systems [1, 2, 3, 4, 5], with action recognition being the most common.

Now, with the growth in popularity of event-based sensors and neuromorphic technologies, a need has arisen for event-based datasets which allow to evaluate such temporal processing capabilities in a neuromorphic set-up.

Inspired by biological vision, event-based sensors (also known as neuromorphic cameras) detect changes in perceived brightness instead of measuring raw brightness [6, 7]. This results in a sparse asynchronous output stream which, compared to a conventional camera, has a much higher temporal resolution, higher dynamic range, robustness to motion blur and lower bandwidth usage. These unique properties open the door for the development of new algorithms that can exploit them. In the machine learning domain, Spiking Neural Networks (SNNs) have been a popular choice for the handling of this data [8, 9], as they implement an end-to-end neuromorphic pipeline with a sparse and asynchronous data flow. Alternatively, approaches such as [10] can also make use of the sparsity of events.

Despite the ample variety of conventional frame-based action recognition datasets, the options for event-based action recognition are very limited [11, 8], forcing many researchers to resort to artificially generated datasets, which either convert frame sequences to events [12, 13] or gen-

erate them from simulations [14, 15]. Alternatively, those who want to employ real data from an event camera have mainly resorted to IBM’s DVS Gesture Dataset [8].

In this work, we prove how the action recognition task in the DVS Gesture dataset does not require temporal understanding in order to be solved. Because of this, we propose the DVS-Gesture-Chain (DVS-GC) dataset, a new task that can only be solved by those systems capable of perceiving the ordering of events in time. This new benchmark allows to test the temporal perception of an action recognition system in real event-based data. Additionally our methodology allows to make the task arbitrarily complex in time, allowing to systematically test the limits of a system’s temporal understanding. From here, we proceed to test this temporal understanding in different feed-forward SNNs and non-spiking Artificial Neural Networks (ANNs).

Through the history of deep learning, when solving non-temporal tasks, feed-forward neural networks such as the Multilayer Perceptron (MLP) or Convolutional Neural Networks (CNNs) have achieved state of the art results in multiple occasions. On the contrary, when the task needs temporal understanding, specialized structures such as recurrent connections need to be used in order to allow for spatio-temporal feature extraction. In this work we explore how certain feed-forward networks can successfully learn temporal dependencies without the use of these structures. In particular, we show how Spiking Neurons have an inherent recurrency that allows them to solve temporal tasks without the aid of recurrent synapses. Additionally, we also analyse the relevance in spatio-temporal feature extraction of time-dependent synaptic weights (TW), Batch Normalization (BN) [16] and Batch Normalization Through Time (BNTT) [17]. The results obtained clarify the role of the aforementioned components in the perception of temporal dependencies. Additionally, this study also serves as performance comparison between SNNs and non-spiking ANNs and helps to elucidate differences in their computing principles.

2 Related work

2.1 Event-based datasets

The event-based sensor market is still in its infancy and its still limited commercial adoption has not allowed to collect large volumes of event-based data yet. Currently, many of the datasets used in machine learning are created artificially from frame-based data or simulations.

One of the proposed ways for the transformation of frames into events has been to perform screen recordings of the target frames. N-MNIST, N-Caltech101 [18] and DVS-CIFAR10 [19] are three neuromorphic classification datasets which were created by recording pre-existing

frame-based datasets with a neuromorphic camera. Mimicking biological vision, these methods created motion by means of saccadic movements which generate the brightness changes required by the neuromorphic camera. In the first two datasets, an Asynchronous Time-based Image Sensor [20] was moved by means of a pan-tilt platform. In the third dataset, a static DVS camera [6] was used, with a moving target image.

Alternatively, frame-based datasets have also been transformed into events directly through software. One example is Pix2NVS [12], a method which creates events by calculating the difference between frames according to their log-intensity/contrast-enhanced values. This was followed by the development of the method by Gehrig et al. [13], which adds an upsampling step and allows to create event sequences with higher temporal resolution. On the other hand, EventGAN [21] proposes an alternative approach which avoids explicitly modelling motion by using a generative adversarial network. These have been applied in some cases [22] to the conversion of action recognition datasets such as UCF-101 [1], but also to tasks such as image classification, object detection, tracking or human pose recognition [13, 21, 23].

Finally, neuromorphic sequences have also been artificially generated through simulators such as [24, 25].

Still, the most desirable option for the development of event-based systems is to use data from a real world acquisition. In the present day, most of the available natively neuromorphic datasets are still simple compared to traditional frame-based ones. Among them we can find N-CARS [26] a binary classification dataset, ASL-DVS [27] a 24 class sign language classification task, DHP19 [28] a 33 class pose estimation dataset, and DVS-Gesture [8] the 11 class action recognition dataset.

2.2 Temporal processing

When processing temporal sequences of stimuli, a property of cognitive systems which is considered to be essential for the task is working memory. This kind of memory holds information from previous events and relates it to the ones perceived later, allowing to understand processes that span over time. Many works refer to this kind of memory as a synonym to short-term memory; still, there are arguments to consider them as different concepts [29, 30].

In the neural engineering world, working memory has been historically implemented by recurrent connections creating what we know as Recurrent Neural Networks (RNN). Past the simple implementation of RNNs, more advanced memory cells such as LSTM [31] and LMU [32] were proposed, which further improve the memory capacity of ANNs and its training through backpropagation.

More recently, temporal processing tasks such as se-

quence transduction [33], time series forecasting [34] and video action recognition [35] have been solved by the increasingly popular attention networks and their Transformer architectures [36]. When using these networks, temporal events are not presented in a succession as they happen, instead, multiple time-steps are accumulated (or the whole sequence in many cases) and then processed offline by the system. These approaches can be considered to implement working memory outside of the neural network by accumulating stimuli through time and then feeding them to the network together as a single input. In the present day, Transformer based ANNs are the most accurate systems for the majority of temporal tasks.

Nevertheless, conventional ANNs still suffer from several shortcomings when compared to real brains, which demonstrate superior computational efficiency, generalisation power and continual learning capabilities. Consequently, as an attempt to capture more of the valuable properties of the brain, the fields of computational neuroscience and artificial intelligence have joined forces by developing biologically inspired SNNs for machine learning tasks. The usage of SNNs brings great gains in energy efficiency when implemented in neuromorphic hardware [37]. Apart from that, they are an appealing option for the processing of neuromorphic inputs such as event camera data, thanks to their sparse and asynchronous computations and their temporal dynamics.

When using SNNs for temporal tasks, the state of the art is still based on conventional RNN architectures. The authors in [38] proposed Recurrent SNNs (RSNNs) of Leaky integrate-and-fire (LIF) neurons with neuronal adaptation, a process that reduces the excitability of neurons based on preceding firing activity. Their resulting network is tested in the Sequential MNIST (S-MNIST) and TIMIT tasks. After that, later work applied LSTM cells to SNN networks achieving higher performance in S-MNIST [39].

Still, for the processing of visual datasets such as DHP19 or DVS-Gesture, the state of the art is set by feed-forward SNNs with no recurrence [40, 41, 42]. The remaining question is then whether these feed-forward SNNs implement working memory or, by the contrary, the aforementioned tasks do not require a temporal understanding. The experiments presented in this work will prove how both statements are true.

3 Methodology

3.1 DVS Gesture Chain dataset

The objective of our new dataset is to define an action recognition task on event-based sequences that requires to have an understanding of temporal dependencies when solving it. In order to have such temporal dependencies, the

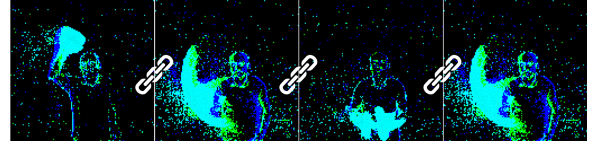


Figure 1. Example frames of a DVS-GC sequence of 90 frames. The user is shown performing 4 gestures in succession. From left to right: Right hand wave, right arm clockwise, air drums and right arm clockwise.

sequences to classify should be composed of a succession of smaller actions, then, the ordering of this sub-actions will have a relevant meaning for the final classification.

The DVS-GC dataset achieves these requirements by leveraging the DVS-Gesture dataset and combining its gestures into chains of gestures. The result is a dataset where the classes to recognise are successions of multiple gestures and the order in which they appear is essential to its correct classification (Fig. 1).

3.1.1 Creation of the action classes

The original DVS-Gesture dataset contains 1,342 instances divided in 11 different gestures, each with 122 trials. Those trials were collected from 29 subjects under 3 different lighting conditions. Using these, the creation of the classes in the new DVS-GC is dependent only of two parameters, i.e. the number of used gestures N and the length of the gesture chain L . Then the number of generated classes C will be equal to all the possible combinations:

$$C = N^L \quad (1)$$

Following this methodology, we can create sequences of arbitrary length L using a number of gestures $N \leq 11$. This allows for a systematic evaluation of the temporal understanding of a system, as the user can now control the temporal complexity of the task by setting N and L .

Still, the training time and computational resources needed will increase as C increases, meaning that the maximum affordable C will be dictated by the available hardware. In order to reduce the number of generated classes without reducing N or L , we also provide an alternative class generation method which does not allow to repeat the same gesture in consecutive positions of the chain. This results in a reduction of the possible permutations of the chain. The number of classes will now be calculated as seen in Eq. 2:

$$C = N(N - 1)^{L-1} \quad (2)$$

Using different values of N , L and the methodology with and without repetition, we created different datasets that we

use to evaluate our networks (results shown in the experiments section).

3.1.2 Chaining of events

Given the stream of 4-dimensional events (x, y, time, polarity) provided by the DVS-Gesture dataset, as done in most state of the art systems [43, 40, 44, 45], we transform them into frames by accumulating events in a time window. The number of generated frames F per sequence is user determined and will be constant for all the instances in the dataset. The resulting frames have two channels, one for positive polarity and one for negative.

Given that the gesture instances are obtained from a set of users under different lighting conditions, the gesture chains are created combining the gestures from the same user under the same lighting condition. This avoids having sudden changes in illumination or the appearance of the user which could help the system to identify the transition between a gesture and the next. Additionally, having a constant number of frames for each gesture in the gesture chain can also allow the machine to know when the transition will happen. To solve this, the duration in frames of each gesture F_g is made variable. Let F be the initial number of frames the gesture sequences have and F_{total} the target number of frames for the final gesture chains, which is user defined. Then, as seen in Eq. 3, the duration of each gesture F_g will be a fraction of F (parametrized by the coefficients α_1 and α_2) which fulfills that the total sum equals F_{total} .

$$\{F_g \in [\alpha_1 F, \alpha_2 F] \mid \sum_{g=1}^L F_g = F_{total}\} \quad (3)$$

Then, the value for F_g is chosen randomly from the set we just defined, and the resampling from F to F_g is done by taking the first F_g frames of the original sequence. We implement this using $\alpha_1 = 0.5$ and $\alpha_2 = 0.7$, which works well when using the sequences in DVS-Gesture because each gesture is repeated several times per recording and therefore it is recognizable even after discarding half of the sequence.

Finally, when targeting a specific F_{total} , the number of initial frames F which will allow the values of F_g to have a uniform distribution between $\alpha_1 F$ and $\alpha_2 F$ is given by Eq. 4:

$$F = \frac{F_{total}}{L} \frac{2}{\alpha_1 + \alpha_2} \quad (4)$$

Looking at the final result, it is noticeable that, because the subjects were recorded performing the gestures in a sequence, the chaining of actions in this dataset is particularly smooth, avoiding sudden scene changes between the concatenated gestures.

3.2 Neural network architecture

For our experiments, we make use of the state of the art SNN system presented in [45], the S-ResNet. Additionally, we also define a non-spiking version of the same architecture for comparison.

The neurons in the SNN are defined by the LIF neuron model. Let i be a post-synaptic neuron, $u_{i,t}$ its membrane potential, $o_{i,t}$ its spiking activation and λ the leak factor (which we set to 0.874 following [45]). The index j represents the pre-synaptic neuron and the weights $w_{i,j}$ dictate the value of the synapses between neurons. Then, the iterative update of the neuron activation is calculated as follows:

$$o_{i,t} = g \left(\sum_j (w_{i,j} o_{j,t}) + \lambda \cdot u_{i,t-1} \right) \quad (5)$$

where $g(x)$ is the thresholding function, which converts voltage to spikes:

$$g(x) = \begin{cases} 1, & \text{if } x \geq U_{th} \\ 0, & \text{if } x < U_{th} \end{cases} \quad (6)$$

After spiking, a reset is performed by the subtraction $u_{i,t}^* = u_{i,t} - U_{th}$, where $u_{i,t}^*$ is the membrane potential after resetting.

As defined in [45], we use a Spikes to Spikes (S2S) implementation for the residual connection and the output layer is defined as a layer without leakage ($\lambda = 1$) and without spiking activation ($U_{th} = \infty$). This output layer accumulates the network output through all time-steps and its voltage $u_{i,T}$ at the last time-step $t = T$ provides the final class scores (Eq. 7). At training time, these are compared to the ground truth labels by means of a cross-entropy loss and the network is trained by Backpropagation Through Time (BPTT), using Stochastic Gradient Descent with a momentum of 0.9.

$$u_{i,T} = \sum_t^T \sum_j (w_{i,j} o_{j,t}) \quad (7)$$

Given the non-differentiability of the thresholding function, a triangle shaped surrogate gradient is used as its derivative (Eq. 8). We use $\alpha = 0.3$.

$$\frac{\partial o_{t,i}}{\partial u_{t,i}} = \alpha \max\{0, 1 - |u_{t,i}|\} \quad (8)$$

Apart from that, the S-ResNet uses BNNT as normalization strategy. As seen in Eq. 9, for a time-dependent input of d dimensions $x_t = (x_{1,t}, \dots, x_{d,t})$, the method defines an individual BN module per time-step. This not only normalizes each feature k (or convolutional channel in the case of

CNNs) independently, as regular BN would do, but also defines independent statistics (mean $\mu_{k,t}$ and standard deviation $\sigma_{k,t}$) and learnable weights ($\gamma_{k,t}$ and $\beta_{k,t}$) per time-step t .

$$BNTT(x_{k,t}) = \gamma_{k,t} \frac{x_{k,t} - \mu_{k,t}}{(\sigma_{k,t})^2 + \epsilon} + \beta_{k,t} \quad (9)$$

On the other hand, for the non-spiking ANN, instead of a neuron model we use the Rectified Linear Unit (ReLU) activation function and we substitute BNTT for regular BN. With these changes, the network becomes a conventional feed-forward ResNet. These networks process the input instantaneously, without temporal dynamics, which means that, for a sequence classification task such as action recognition, they can give an output per time-step but not a global one for the whole sequence. We solve this by adding the same output layer used by the SNN, which can be seen as a voting system that accumulates the outputs for all time-steps by summing them together (Eq. 7). With this, we allow a system without temporal processing capabilities to be evaluated in temporal tasks.

4 Experiments

In this section, we prove how a network without the capability for temporal feature extraction can solve the classification task in DVS-Gesture, but fails to do so in the new DVS-GC, which demands a perception of temporal order. Then, we solve DVS-GC with different SNNs and ANNs that implement temporal perception and we analyse which computational units are enabling this capacity. Specifically, we study the contribution of spiking neurons, time-dependent synaptic weights, BN and BNTT. Training was performed using 4 Nvidia GeForce GTX 1080 Ti GPUs.

4.1 DVS-Gesture evaluation

Many previous works reporting accuracy performances in DVS-Gestures have taken the approach of training with the whole training set, evaluating test set performance through training epochs and then reporting the accuracy of the best performing epoch as the final test accuracy. We consider this approach to be reporting validation accuracy rather than test. Therefore, in our setup, we evaluate the test set after all the training epochs, without using its value for tuning the training.

Table 1 shows how both the SNN (S-ResNet38) and ANN (ResNet38) manage to solve the DVS-Gestures task with high accuracy. As previously stated, the ANN final prediction is just a sum of the individual predictions made at each time-step. Each of these is made using the information from a frame which contains multiple events collected from a time window; in the case of our experiments, the

Table 1. Action recognition test performance on DVS-Gesture. SNN stands for an S-Resnet38 with 32 base filters and ANN stands for its non-spiking version. SNN* was initialized with pre-trained weights. Training and testing were run for 3 times, accuracies presented as mean \pm std.

| Network | Normalization | DVS-Gesture Accuracy |
|---------|---------------|----------------------|
| SNN | BN | 70.31 \pm 3.27 % |
| SNN | BNTT | 89.82 \pm 1.50% |
| SNN* | BNTT | 94.84 \pm 1.06 % |
| ANN | BN | 97.35 \pm 0.45 % |
| ANN | BNTT | 96.95 \pm 0.61% |

time window is $\frac{1}{50}$ of the total event sequence. Because the ANN has no way of combining information from other frames and because it has no notion of the timing in where frames happened, this means that the spatial information in the DVS-Gesture events is enough to solve the task and it is not necessary to interpret their ordering or correlation in time. This implies that the action recognition task in DVS-Gesture does not evaluate temporal understanding and it can be solved by systems designed for the classification of static images.

Additionally, we also report the accuracy obtained by the SNN with conventional BN and the accuracy of the ANN with BNTT. It can be seen how the ANN does not benefit from the time-dependent computations of BNTT and obtains a very similar result. On the contrary, the SNN performance decreases dramatically when using regular BN, demonstrating how time agnostic normalization does not suit the temporal dynamics in spiking neurons. This behaviour is to be expected given that their statistics vary between time-steps.

Finally, we also test the performance of the SNN with pre-trained weights used as initialization. As proposed in [45], the network is pre-trained with the CIFAR-100 image classification dataset. This results in a higher final accuracy compared to training from scratch; but still the final accuracy obtained by the ANN is higher than the one of the SNN.

4.2 DVS-Gesture-Chain evaluation

Using the methodology described in the previous section 4.2 we created three DVS-GC datasets. The first using $N = 3$, $L = 6$ and the method without repetition (Eq. 2), which results in 96 classes. The other two using $N = 3$, $L = 4$ and the method with repetition (Eq. 1), which results in 81 classes. One of these 81-class datasets was created with $\alpha_1 = 0.2$ and $\alpha_1 = 1$ (the rest use the standard $\alpha_1 = 0.5$ and $\alpha_1 = 0.7$).

For these datasets we create a validation set with 20% of the training data and we evaluate it at every epoch. The test performance is then evaluated using the weights with highest validation accuracy.

As seen in Table 2, now that the task requires to distinguish the ordering of the events, the non-temporal ANN fails to solve it. Moreover, its accuracy value implicitly reveals the computations performed by the network. Taking the 81 class dataset as example, one can see how the ANN accuracy ($16.91\% \pm 0.5$) is higher than random chance (1.23%). This is because the network is capable of detecting the gestures present in the sequence and the number of times they appear, but it is unable to perceive their ordering. With such conditions, and assuming a perfect accuracy in gesture detection, the probability to correctly classify a sequence for the 81 class dataset is $p_d = 16.05\%$. We obtain this value by calculating the probability to correctly classify each individual class x_i in the dataset and then computing the average among them (Eq.10):

$$p(x) = \begin{cases} 1, & \text{if gesture repeated 4 times} \\ \frac{1}{4}, & \text{if gesture repeated 3 times} \\ \frac{1}{6}, & \text{if 2 gestures repeated 2 times} \\ \frac{1}{36}, & \text{otherwise} \end{cases}$$

$$P_d = \frac{1}{C} \sum_i^C p(x_i) =$$

$$= \frac{1}{81} (3 \cdot 1 + 24 \cdot \frac{1}{4} + 18 \cdot \frac{1}{6} + 36 \cdot \frac{1}{36}) = 0.1605 \quad (10)$$

On the other hand, the results show how the SNN still achieves high accuracy on DVS-GC, implying that its temporal dynamics allow to perceive temporal ordering. In order to analyse which components of the network are enabling temporal understanding, we also test the performance of the SNN with conventional BN and the accuracy of the ANN with BNTT. The accuracies obtained by both systems indicate that these networks are successfully learning to perceive order, meaning that both, spiking neurons and BNTT can enable a neural network to learn temporal perception on their own. Additionally, it is also worth noticing how, for this task, the ANN with BNTT is more accurate than the SNN.

In BNTT, the temporal perception capabilities are gained by learning time-dependent values that are used to scale the activation maps of the network (further detail given in the next section). In order to decorrelate this capacity from the normalization strategy, we create a modified version of the non-temporal ANN with regular BN that we call ANN-TW (ANN with temporal weight). This version adds a learnable weight $w_{l,t} \in \mathbb{R}^1$ per time-step t at each layer l , which is used to scale the activation map after the convolution

Table 2. Test performance on DVS-GC. SNN stands for an S-Resnet38 with 32 base filters and ANN stands for its non-spiking version. Training and testing were run for 3 times, accuracies presented as mean \pm std. Classes indicates which of the 2 generated datasets was used.

| Network | Normalization | Classes | Accuracy |
|---------|---------------|---------|--------------------|
| ANN | BN | 81 | $16.91 \pm 0.5\%$ |
| ANN | BNTT | 81 | $99.52 \pm 0.31\%$ |
| ANN | None | 81 | 1.24 % |
| SNN | BN | 81 | $80.02 \pm 2.5\%$ |
| SNN | BNTT | 81 | $95.83 \pm 0.62\%$ |
| SNN | None | 81 | 1.24 % |
| ANN-TW | BN | 81 | $89.44 \pm 5.74\%$ |
| ANN-TWC | BN | 81 | $91.08 \pm 8.10\%$ |
| ANN | BN | 96 | $12.96 \pm 0.74\%$ |
| ANN | BNTT | 96 | $99.52 \pm 0.55\%$ |
| SNN | BN | 96 | $80.62 \pm 2.76\%$ |
| SNN | BNTT | 96 | $96.32 \pm 0.02\%$ |

(Conv) and BN layers:

$$y_{l,t} = BN(Conv(x_{l,t})) \cdot w_{l,t} \quad (11)$$

Apart from that, the weights learned in the ANN-TW are shared across the channel dimension. On the contrary, in the case of BNTT, the values are learned independently per channel.

The performance of ANN-TW (Table 2) proves how a single time-dependent weight per layer is enough to perceive temporal order and how the learned value does not need to be different between channels of the same layer. Additionally, we also compare to a version with independent weights per channel (ANN-TWC), which obtains similar results but proves how channel dependent weights are slightly more accurate. Apart from that, the performances of both networks are lower to that of the systems using time-dependent normalization statistics, proving how these are not essential but indeed beneficial.

As a final test, we also evaluate the performances of the networks with a modified DVS-GC where the value of the coefficients in equation 3 is changed to $\alpha_1 = 0.2$ and $\alpha_2 = 1$. This gives more variability to the duration F_g of each individual gesture and makes it much harder to predict where the transition between gestures will happen. The results in Table 3 demonstrate how this new setup vastly decreases the performance of the ANN-BNTT. In contrast, SNN-BNTT exhibits a smaller decrease and still solves the task with relatively high accuracy. The reason behind these results is elucidated in the following section.

Table 3. Test performance on the 81 class DVS-GC with $\alpha_1 = 0.2$ and $\alpha_1 = 1$. This dataset has unpredictable time-windows for the appearance of gestures in the chain. SNN stands for an S-Resnet38 with 32 base filters and ANN stands for its non-spiking version.

| Network | Normalization | Accuracy |
|---------|---------------|--------------------|
| ANN | BNTT | $61.14 \pm 0.35\%$ |
| SNN | BNTT | $80.24 \pm 0.92\%$ |

Table 4. Test accuracy of the ANN-BNTT after averaging certain components through time. "Non-averaged components" indicates which parts have not been averaged and therefore are still time-dependent.

| Non-averaged components | Accuracy |
|-------------------------|----------|
| Full BNTT | 99.16 % |
| β weight | 97.63 % |
| γ weight | 93.77 % |
| Variance | 72.24 % |
| Mean | 35.96 % |
| None | 17.09 % |

4.2.1 BNTT Ablation study

The BNTT module has 4 time-varying parameters, namely mean, variance, γ weight and β weight. In order to analyse their role in temporal understanding, we perform an ablation study where we eliminate the temporal dimension of some of this components by averaging across all time-steps. This allows to isolate the temporal performance of individual components and evaluate the accuracy degradation. Notice that the experiment is performed by first training the regular network and then averaging the necessary parameters, with no retraining after the ablation.

Table 4 presents the results for each of the 4 BNTT parameters in isolation (all the other parameters were averaged in time). It can be seen how any of them is enough to maintain accuracy well above 16.05%, meaning that they all capacitate the network to perceive temporal order. Still, there is a clear difference in accuracy between them, with γ and β weights having the highest accuracy and the mean having the lowest one. Of course, after averaging all of them, the network falls back to the performances seen by the ANN with regular BN.

5 Further analysis: How is temporal feature extraction implemented?

After proving through empirical results how spiking neurons, time-dependent weights and time-dependent normali-

zation enable temporal understanding, in this section we analyse the in-depth mechanics that explain how exactly this capability is being implemented.

5.1 time-dependent weight and normalization

Networks with time-dependent weights such as ANN-TW or those using BNTT are able to understand order because they are capable of storing at which time a visual detection happened. This is achieved by constraining the activation of certain layers or channels to a time window, then the feature detected by those neurons will be known to happen within that time-window.

In order to prove how the networks learn to use the aforementioned logic, we visualize the value of the temporal weight in ANN-TW (Fig. 2.B) and the value of the β weight in ANN-BNTT (Fig. 2.A) through time. For the BNTT weight, as the value also varies between channels of the same layer, we plot their average.

First, notice that, when designing DVS-GC, we made the gesture chaining procedure variable in time, so that the transition between gestures does not always happen in the same time-step. Now, visualizing the graphs, it can be seen how the networks learned to reduce the weight in the uncertainty zone of the transition and defined their detection time windows between the time-steps which are guaranteed to belong to the n -th gesture.

Then, among those time windows, it can be seen how the difference in value is very small for the β weight, while ANN-TW displays large changes. This is because the β weight has a different value per channel, therefore the network learned to associate different time windows per channel, something that is not visible in Fig. 2.A. On the contrary, the weight in ANN-TW shares the same value for all channels, therefore it associates the same time-window to the whole layer. This behaviour is clearly seen in Fig. 2.B, where the layers are restricted to only be active in the time windows corresponding to certain positions in the 4-gesture chain. Like this, each layer will specialize in detecting gestures at a certain position in the chain.

In order to visualize the temporal windowing of the BNTT weight through channels, in Fig. 2.C we plot the center of mass m in the time dimension for the weights at each channel.

Let $x = (x_1, \dots, x_T)$ be a vector that contains a weight value x_t per time-step t . Then, m is calculated as:

$$m = \frac{1}{T} \sum_t^T (x_t - \min(x))t \quad (12)$$

With a uniform distribution of weight through the time-steps, the center of mass would have a value equal to $T/2$, which in the case of our network would be 30. Consequently, all those values in Fig. 2.C which are far from

this number are indicators of the existence of a time window. Moreover, it can be seen how the center of mass varies among different channels, demonstrating how they specialize on detecting features inside different temporal windows.

In conclusion, these networks implement temporal order perception by associating timestamps to the features they detect and then combining this information in the last layer by accumulation. This last layer is the only element in the system implementing memory.

Given this computational logic, it is then clear why in Table 3, the performance of these networks dropped. With $\alpha_1 = 0.2$ and $\alpha_1 = 1$, in a chain of 4 gestures, there is no time-step in the sequence guaranteed to contain the second or third gesture, as the transition zones now overlap. Visualizing the value of the β weight for an ANN with BNNTT, in Fig. 3 we can observe how the network learns to give higher importance to the first and last time-steps, which are guaranteed to belong to the first and last gesture, but does not find relevant time-steps for the middle gestures.

5.2 Spiking neuron

Spiking neurons are, by definition, computing units with memory. The input voltage they receive is accumulated through time, therefore, they store information. Thanks to this property, a feed-forward SNN without temporal weights is able to learn temporal order perception, as proven by our experiments.

In this work, we use a LIF neuron model with reset by subtraction (Fig. 4). This neuron can be seen as a recurrent unit where the previous state v_{t-1} is summed to the current input x_t . The contribution of v_{t-1} is weighted by the leak factor λ and the final voltage v_t is decreased by subtracting V_{res} in the event of a spike. These mechanisms fulfil a very similar purpose than the gating mechanisms present in other recurrent units such as LSTM, they control how to forget previous information. The main difference is that an LSTM cell comprises all neurons in a layer and uses all their information to calculate gating coefficients by means of learnable layers. On the contrary, the recurrence of a spiking neuron happens within each neuron individually and forgetting depends only on its own spike events and the fixed value λ . Still, through inhibitory connections, the network can learn to implement other forgetting strategies.

Therefore, even when not equipped with recurrent connections, a network of spiking neurons can potentially learn to combine information from different time-steps in order to detect time invariant spatio-temporal features, such as the transition from one gesture to another in DVS-GC. This would justify why SNNs can maintain high accuracy even where temporal weights fail (Table 3). Alternatively, for tasks such as the ones in Table 2, a feed-forward SNN could also learn to keep a record of how many events have oc-

Table 5. Test accuracy of the SNN with conventional BN with and without leak factor. Training and testing were run for 3 times, accuracies presented as mean \pm std.

| Leak | Accuracy |
|-------------------|--------------------|
| $\lambda = 0.874$ | $80.02 \pm 2.5\%$ |
| $\lambda = 1$ | $48.27 \pm 1.38\%$ |

curred since the beginning of the sequence and combine this information with spatial features to perceive the order in which events happen.

As a final test, we evaluate the influence of the leak factor in the network's performance. Table 5 shows how the accuracy of SNN-BN vastly decreases when trained without it. This demonstrates how progressively forgetting old information is of great importance for precise temporal computations. Still, this low accuracy is still enough to prove temporal understanding, indicating that some temporal processing capabilities are still present without leakage.

6 Conclusions

In this work a novel method was proposed which allows to reuse existing event data to generate an action recognition task that is arbitrarily complex in time. The resulting dataset, DVS-GC, allows, for the first time, to measure the capacity of a machine learning system for temporal ordering perception in real event-based video. The experimental results confirmed how the original DVS-Gesture could be solved by systems without temporal perception, unlike the new DVS-GC.

Then, the temporal understanding of feed-forward SNNs and ANNs was tested, proving how spiking neurons, time-dependent weights and BNNTT allow for the perception of temporal ordering. Further analysis unveiled the specific properties that allow for this capacity to be implemented. Through this analysis it was demonstrated how time-dependent weights and normalization enable ordering perception only when the time windows containing the relevant events are predictable. On the contrary, spiking neurons do not have this limitation. Additionally, the obtained results also provided other relevant insights: time-dependent normalization statistics improve results when temporal computations are needed, but do not bring benefit when computations are strictly spatial. Forgetting information in spiking neurons through voltage leak is key for temporal computations. For datasets with unpredictable time-windows, ANNs would need to explicitly implement memory in its hidden layers (for example through recurrent connections) to successfully perceive order, while SNNs can

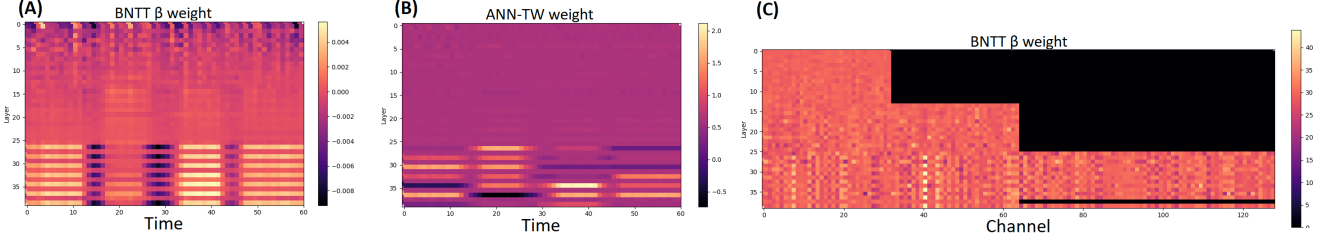


Figure 2. (A):Average Value across channels of the bias weight in the BNNT layers of the ANN with BNNT. Trained in DVS-GC with 81 classes.(B): Value of the time weight in TW-ANN. Trained in DVS-GC with 81 classes. (C): Value of the center of mass in the time dimension (60 time-steps) of the bias weight of the BNNT layers in the ANN with BNNT. The last two layers of all graphs correspond to the layers in the residual connection downsampling.

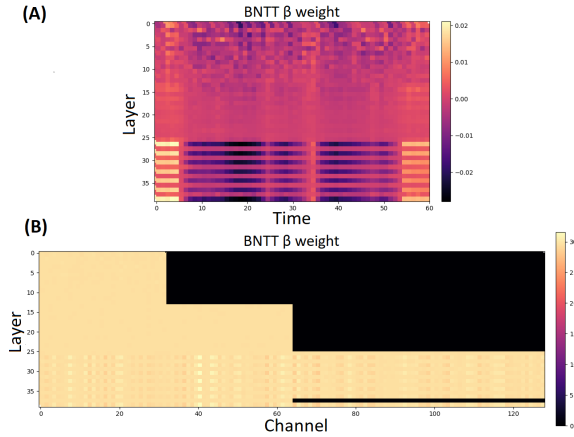


Figure 3. (A):Average Value across channels of the bias weight in the BNNT layers of the ANN with BNNT. (B): Value of the center of mass in the time dimension (60 time-steps) of the bias weight of the BNNT layers in the ANN with BNNT. The last two layers of both graphs correspond to the layers in the residual connection downsampling. Trained in DVS-GC with 81 classes with $\alpha_1 = 0.2$ and $\alpha_1 = 1$.

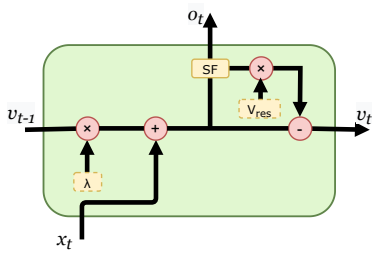


Figure 4. LIF neuron diagram. *SF* stands for spiking function. V_{res} is the voltage reset value.

leverage their inherent memory capabilities. For the DVS-GC datasets with predictable time-windows and within our specific training setup, conventional ANNs displayed higher accuracy than SNNs in event-based action recognition.

Understanding the role of these low-level components in temporal calculations allows to optimize design choices when building spatio-temporal feature extractors. In our case, we proved how, for problems such as the perception of temporal ordering, feed-forward networks can be enabled to solve the task. Still, this does not imply that it is the optimal solution in all cases. As it can be seen in our SNN vs LSTM discussion, RNNs enable more complex temporal computations, and comparing to time-dependent weights, RNNs are not limited to working with a fixed number of time-steps. Therefore for many temporal tasks, recurrent synapses are still the optimal choice.

Apart from that, we believe that comparing different computing paradigms, as we did with ANNs vs SNNs, is necessary in order to understand their similarities and differences, which will allow to further understand intelligence and how to implement it.

Acknowledgement

This work was supported by the US Air Force Office of Scientific Research under Grant for project FA8655-20-1-7037. The contents were approved for public release under case AFRL-2021-3889 and they represent the views of only the authors and does not represent any views or positions of the Air Force Research Laboratory, US Department of Defense, or US Government. The authors declare that there is no conflict of interest.

References

[1] Khurram Soomro, Amir Roshan Zamir, and Mubarak Shah. Ucf101: A dataset of 101 human actions classes from videos

in the wild. *arXiv preprint arXiv:1212.0402*, 2012.

[2] Will Kay, João Carreira, Karen Simonyan, Brian Zhang, Chloe Hillier, Sudheendra Vijayanarasimhan, Fabio Viola, Tim Green, Trevor Back, Apostol Natsev, Mustafa Suleyman, and Andrew Zisserman. The kinetics human action video dataset. *ArXiv*, abs/1705.06950, 2017.

[3] Hilde Kuehne, Hueihan Jhuang, Estíbaliz Garrote, Tomaso A. Poggio, and Thomas Serre. Hmdb: A large video database for human motion recognition. *2011 International Conference on Computer Vision*, pages 2556–2563, 2011.

[4] Antoine Miech, Dimitri Zhukov, Jean-Baptiste Alayrac, Makarand Tapaswi, Ivan Laptev, and Josef Sivic. Howto100m: Learning a text-video embedding by watching hundred million narrated video clips. *2019 IEEE/CVF International Conference on Computer Vision (ICCV)*, pages 2630–2640, 2019.

[5] Fabian Caba Heilbron, Victor Escorcia, Bernard Ghanem, and Juan Carlos Niebles. Activitynet: A large-scale video benchmark for human activity understanding. *2015 IEEE Conference on Computer Vision and Pattern Recognition (CVPR)*, pages 961–970, 2015.

[6] Patrick Lichtsteiner, Christoph Posch, and Tobi Delbrück. A 128 128 120 db 15 s latency asynchronous temporal contrast vision sensor. 2006.

[7] Tobi Delbrück, Bernabé Linares-Barranco, Eugenio Culurciello, and Christoph Posch. Activity-driven, event-based vision sensors. *Proceedings of 2010 IEEE International Symposium on Circuits and Systems*, pages 2426–2429, 2010.

[8] Arnon Amir, Brian Taba, David J. Berg, Timothy Melano, Jeffrey L. McKinstry, Carmelo di Nolfo, Tapan Kumar Nayak, Alexander Andreopoulos, Guillaume Garreau, Marcela Mendoza, Jeffrey A. Kusnitz, Michael V. DeBole, Steven K. Esser, Tobi Delbrück, Myron Flickner, and Dharmendra S. Modha. A low power, fully event-based gesture recognition system. *2017 IEEE Conference on Computer Vision and Pattern Recognition (CVPR)*, pages 7388–7397, 2017.

[9] Paul Kirkland, Davide Manna, Alex Vicente Sola, and Gae-tano Di Caterina. Unsupervised spiking instance segmentation on event data using stdp features. *IEEE Transactions on Computers*, 2022.

[10] Qinyi Wang, Yexin Zhang, Junsong Yuan, and Yilong Lu. Space-time event clouds for gesture recognition: From RGB cameras to event cameras. *Proceedings - 2019 IEEE Winter Conference on Applications of Computer Vision, WACV 2019*, (January):1826–1835, 2019.

[11] Junhaeng Lee, Tobi Delbrück, Michael Pfeiffer, Paul K. J. Park, Chang-Woo Shin, Hyunsuk Ryu, and Byung-Chang Kang. Real-time gesture interface based on event-driven processing from stereo silicon retinas. *IEEE Transactions on Neural Networks and Learning Systems*, 25:2250–2263, 2014.

[12] Yin Bi and Yiannis Andreopoulos. Pix2nvs: Parameterized conversion of pixel-domain video frames to neuromorphic vision streams. *2017 IEEE International Conference on Image Processing (ICIP)*, pages 1990–1994, 2017.

[13] Daniel Gehrig, Mathias Gehrig, Javier Hidalgo-Carri’o, and Davide Scaramuzza. Video to events: Recycling video datasets for event cameras. *2020 IEEE/CVF Conference on Computer Vision and Pattern Recognition (CVPR)*, pages 3583–3592, 2020.

[14] Elias Mueggler, Henri Rebucq, Guillermo Gallego, Tobi Delbrück, and Davide Scaramuzza. The event-camera dataset and simulator: Event-based data for pose estimation, visual odometry, and slam. *The International Journal of Robotics Research*, 36:142 – 149, 2017.

[15] Henri Rebucq, Daniel Gehrig, and Davide Scaramuzza. Esim: an open event camera simulator. In *CoRL*, 2018.

[16] Sergey Ioffe and Christian Szegedy. Batch normalization: Accelerating deep network training by reducing internal covariate shift. In *International conference on machine learning*, pages 448–456. PMLR, 2015.

[17] Youngeun Kim and Priyadarshini Panda. Revisiting batch normalization for training low-latency deep spiking neural networks from scratch. *Frontiers in neuroscience*, page 1638, 2020.

[18] Garrick Orchard, Ajinkya Jayawant, Gregory K Cohen, and Nitish Thakor. Converting static image datasets to spiking neuromorphic datasets using saccades. *Frontiers in neuroscience*, 9:437, 2015.

[19] Hongmin Li, Hanchao Liu, Xiangyang Ji, Guoqi Li, and Luping Shi. Cifar10-dvs: an event-stream dataset for object classification. *Frontiers in neuroscience*, 11:309, 2017.

[20] Christoph Posch, Daniel Matolin, and Rainer Wohlgenannt. A qvga 143 db dynamic range frame-free pwm image sensor with lossless pixel-level video compression and time-domain cds. *IEEE Journal of Solid-State Circuits*, 46(1):259–275, 2010.

[21] Alex Zihao Zhu, Ziyun Wang, Kaung Khant, and Kostas Daniilidis. Eventgan: Leveraging large scale image datasets for event cameras. In *2021 IEEE International Conference on Computational Photography (ICCP)*, pages 1–11. IEEE, 2021.

[22] Aaron Chadha, Yin Bi, Alhabib Abbas, and Yiannis Andreopoulos. Neuromorphic vision sensing for cnn-based action recognition. In *ICASSP 2019-2019 IEEE International Conference on Acoustics, Speech and Signal Processing (ICASSP)*, pages 7968–7972. IEEE, 2019.

[23] Cian Ryan, Brian O’Sullivan, Amr Elrasad, Aisling Cahill, Joe Lemley, Paul Kiely, Christoph Posch, and Etienne Perot. Real-time face & eye tracking and blink detection using event cameras. *Neural Networks*, 141:87–97, 2021.

[24] Henri Rebucq, Daniel Gehrig, and Davide Scaramuzza. ESIM: an open event camera simulator. *Conf. on Robotics Learning (CoRL)*, October 2018.

[25] Damien Joubert, Alexandre Marcireau, Nic Ralph, Andrew Jolley, André van Schaik, and Gregory Cohen. Event camera simulator improvements via characterized parameters. *Frontiers in Neuroscience*, page 910, 2021.

[26] Amos Sironi, Manuele Brambilla, Nicolas Bourdis, Xavier Lagorce, and Ryad Benosman. Hats: Histograms of averaged time surfaces for robust event-based object classification. In *Proceedings of the IEEE Conference on Computer Vision and Pattern Recognition*, pages 1731–1740, 2018.

[27] Yin Bi, Aaron Chadha, Alhabib Abbas, Eirina Bourtsoulatze, and Yiannis Andreopoulos. Graph-based object classification for neuromorphic vision sensing. In *Proceedings of the IEEE/CVF International Conference on Computer Vision*, pages 491–501, 2019.

[28] Enrico Calabrese, Gemma Taverni, Christopher Awai Easthope, Sophie Skribine, Federico Corradi, Luca Longinotti, Kynan Eng, and Tobi Delbrück. Dhp19: Dynamic vision sensor 3d human pose dataset. In *Proceedings of the IEEE/CVF conference on computer vision and pattern recognition workshops*, pages 0–0, 2019.

[29] Adele Diamond. Executive functions. *Annual review of psychology*, 64:135–168, 2013.

[30] Nelson Cowan. What are the differences between long-term, short-term, and working memory? *Progress in brain research*, 169:323–338, 2008.

[31] Sepp Hochreiter and Jürgen Schmidhuber. Long short-term memory. *Neural computation*, 9(8):1735–1780, 1997.

[32] Aaron Voelker, Ivana Kajić, and Chris Eliasmith. Legendre memory units: Continuous-time representation in recurrent neural networks. *Advances in neural information processing systems*, 32, 2019.

[33] Sho Takase and Shun Kiyono. Lessons on parameter sharing across layers in transformers. *arXiv preprint arXiv:2104.06022*, 2021.

[34] Haoyi Zhou, Shanghang Zhang, Jieqi Peng, Shuai Zhang, Jianxin Li, Hui Xiong, and Wancai Zhang. Informer: Beyond efficient transformer for long sequence time-series forecasting. In *Proceedings of AAAI*, 2021.

[35] Chen Wei, Haoqi Fan, Saining Xie, Chao-Yuan Wu, Alan Yuille, and Christoph Feichtenhofer. Masked feature prediction for self-supervised visual pre-training. *arXiv preprint arXiv:2112.09133*, 2021.

[36] Ashish Vaswani, Noam Shazeer, Niki Parmar, Jakob Uszkoreit, Llion Jones, Aidan N Gomez, Łukasz Kaiser, and Illia Polosukhin. Attention is all you need. *Advances in neural information processing systems*, 30, 2017.

[37] Mike Davies, Andreas Wild, Garrick Orchard, Yulia Sandomirskaya, Gabriel A Fonseca Guerra, Prasad Joshi, Philipp Plank, and Sumedh R Risbud. Advancing neuromorphic computing with loihi: A survey of results and outlook. *Proceedings of the IEEE*, 109(5):911–934, 2021.

[38] Guillaume Bellec, Darjan Salaj, Anand Subramoney, Robert Legenstein, and Wolfgang Maass. Long short-term memory and learning-to-learn in networks of spiking neurons. *Advances in neural information processing systems*, 31, 2018.

[39] Ali Lotfi Rezaabad and Sriram Vishwanath. Long short-term memory spiking networks and their applications. In *International Conference on Neuromorphic Systems 2020*, pages 1–9, 2020.

[40] Hanle Zheng, Yujie Wu, Lei Deng, Yifan Hu, and Guoqi Li. Going deeper with directly-trained larger spiking neural networks. In *AAAI*, 2021.

[41] Wei Fang, Zhaofei Yu, Yanqi Chen, Tiejun Huang, Timothée Masquelier, and Yonghong Tian. Deep residual learning in spiking neural networks. *Advances in Neural Information Processing Systems*, 34, 2021.

[42] Youngeun Kim and Priyadarshini Panda. Optimizing deeper spiking neural networks for dynamic vision sensing. *Neural Networks*, 144:686–698, 2021.

[43] Jacques Kaiser, Hesham Mostafa, and Emre Neftci. Synaptic plasticity dynamics for deep continuous local learning (decolle). *Frontiers in Neuroscience*, 14:424, 2020.

[44] Wei Fang, Zhaofei Yu, Yanqi Chen, Timothée Masquelier, Tiejun Huang, and Yonghong Tian. Incorporating learnable membrane time constant to enhance learning of spiking neural networks. In *Proceedings of the IEEE/CVF International Conference on Computer Vision*, pages 2661–2671, 2021.

[45] Alex Vicente Sola, Davide Liberato Manna, Paul Kirkland, Gaetano Di Caterina, and Trevor J Bihl. Keys to accurate feature extraction using residual spiking neural networks. *Neuromorphic Computing and Engineering*, 2022.